Suppressing chaos in a simplest autonomous memristor-based circuit of fractional order by periodic impulses

Marius-F. Danca[a,b], Wallace K. S. Tang[c], Guanrong Chen[c,*]

[a] *Dept. of Mathematics and Computer Science, Avram Iancu University of Cluj-Napoca, Romania*
[b] *Romanian Institute of Science and Technology, 400487 Cluj-Napoca, Romania*
[c] *Department of Electronic Engineering, City University of Hong Kong, Hong Kong*

Abstract

In this paper, the chaotic behavior of a simplest autonomous memristor-based circuit of fractional order is suppressed by periodic impulses applied to one or several state variables. The circuit consists of two passive linear elements, a capacitor and an inductor, as well as a nonlinear memristive element. It is shown that by applying a sequence of adequate (identical or different) periodic impulses to one or several variables, the chaotic behavior can be suppressed. Impulse values and control timing are determined numerically, based on the bifurcation diagram with impulses as bifurcation parameters. Empirically, the probability to have a reasonably wide range of impulses to suppress chaos is quite large, ensuring that chaos suppression can be implemented, as demonstrated by several examples presented.

Keywords: Memristor; Chaos suppression; Impulsive fractional-order system

1. Introduction

The simplest autonomous memristor-based chaotic circuit (SCC) of integer order, presented by Muthuswamy and Chua in [1], consists of only three circuit elements. As shown in Fig. 1, there are two energy-storage passive and linear elements (an inductor and a capacitor), and a nonlinear active memristor. In this way, the required circuit elements to generate chaos reduces to three, giving "the simplest possible circuit in the sense that we also have only one *locally-active* element, the memristor" [1] (see [2] for the notion of local activity).

The existence of memristor was stipulated by Chua in 1971 in his seminal paper "The missing circuit element" [3]. From a circuit-theoretic point of view, he postulated that there are four fundamental circuit variables, namely the voltage v, charge q, flux linkage φ and current i, and six two-variable combinations of those elements, as shown in Table 1 [3, 4]. "From the logical as well as axiomatic points of view, it is necessary for the sake of completeness to postulate the existence of a fourth basic two-terminal circuit element which is characterized by a $\varphi - q$ curve" [3], filling the missing nonlinear relationship between charge q and flux φ, $M(\varphi, q) = 0$ (Table 1).

The term *memristor*, coined by Chua, also reflects the fact that it behaves somewhat like a nonlinear resistor with memory.

The real existence of this device was established in 2008, when a physical prototype of a two-terminal device behaving as memristor was announced in Nature [5], after Williams's group in the

*Corresponding author

Combinations of $q,\ v,\ \varphi,\ i$	Relationships
(v, i)	$v = Ri$
(φ, i)	$\varphi = Li$
(q, i)	$q(t) = \int_{-\infty}^{t} i(\tau)d\tau$
(q, v)	$q = Cv$
(φ, v)	$\varphi = \int_{-\infty}^{t} v(\tau)d\tau$
(φ, q)	memristor: $M(\varphi, q) = 0$

Table 1: Six possible 2-variable relationships.

HP Labs reported it on 30 April 2008. They proved the existence of a fourth basic element in integrated circuits by realizing the world-first memristor, characterizing the memristor as being "a contraction of memory resistor, because that is exactly its function: to remember its history".

As shown by Chua, memristor can replace a circuit of over 15 transistors and several other passive elements, especially in small (molecular or cellular) scales. Therefore, it is useful for a large number of potential applications, generating great interest from the scientific community. For example, behaving functionally like synapses, memristors could be utilized in analog circuits mimicking the functions of the human brain (see e.g. [4]). Today, there are many research groups working on similar projects, for example, IBMs Blue Brain project, Howard Hughes Medical Institute's Janelia Farm, and Harvard Center for Brain Science. There are also many other applications in various areas, such as in electric circuits [6], logic circuits [7], concepts of computer memory [8], DRAM, flash, and disks [9], electroforming of metals and semiconductor oxides [10], memristor networks [11], bioelectricity modeling [12], next generation computers [13], cellular automata [11], linearized model of the pinched $i - v$ hysteresis [14], to mention only a few (more references can be found in [15]). The increasing interest in this element is strongly justified by the fact that more than 1800 papers published on the topic up to the middle of 2015 according to the Web of Science. It is also remarked that the concept of memristor was extended by Chua to the memcapacitor and meminductor [16], which also generate a lot of excitement to the field.

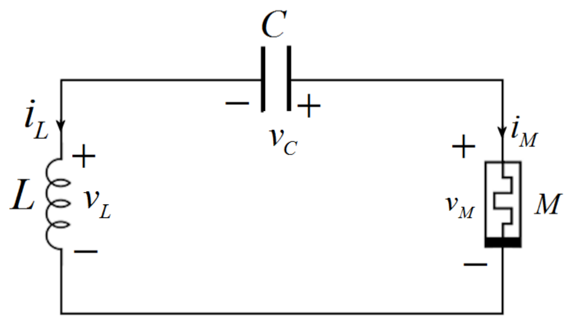

Figure 1: Simplest autonomous memristor-based chaotic circuit, as presented in [1].

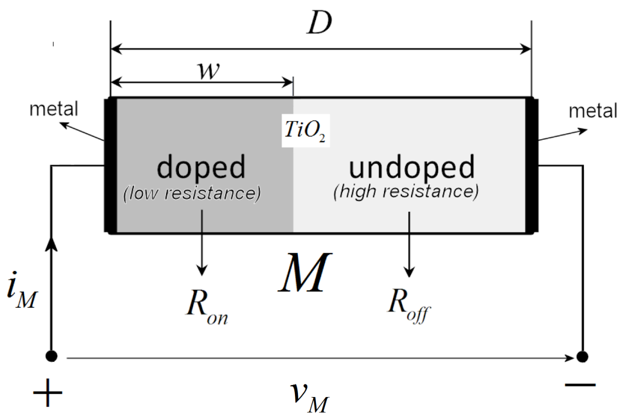

Figure 2: Scheme of titanium-dioxide (TiO_2) memristor (adapted from [5]).

Here, consider the *current-controlled* (or *charge-controlled*) *ideal memristor* [3] (Fig. 2), as presented by the HP group, which is modeled by the following port and state equations respectively [5] (similarly, *voltage-controlled* memristor equations can be defined [17]):

$$M : \begin{cases} v_M(t) = R(x(t))i_M(t), & \text{(1a)} \\ \dot{x}(t) = \pm k f(x(t)) i_M(t). & \text{(1b)} \end{cases}$$

In this model, $R(x)$, called the *memristence* [3] as defined for HP's memristor [5], is a sum of the resistances of the doped and undoped regions (Fig. 2):

$$R(x) = xR_{on} + (1-x)R_{off}, \quad x = \frac{w}{D} \in (0,1), \tag{2}$$

where x represents the internal state memristor variable, with w being the width of the doped region, referenced to as the total length D ($\approx 10nm$) of the (TiO_2-based) semiconductor film sandwiched between two metal contacts [5][1]; R_{on} and R_{off} ($R_{on} \ll R_{off}$) are the minimum and the maximum resistances respectively, to which the device can be configured (corresponding to $w = 0$ and $w = D$ respectively, see also [6, 19]). In (1b), $f(x)$ is the so-called dopant drift window function, which models the internal state of the memristor, and k depends directly proportional to R_{on} and inversely proportional to D, while $\pm$ represents the memristor polarity [5].

Hereafter, for notational simplicity, unless necessary the time argument t will be dropped.

The nonlinear scalar function f defined in (1b), is necessary to compensate the differences between the experimental model and the theoretical model. Function f is continuous with which the solution existence and uniqueness of the underlying state equation are ensured. Several variants of f have been proposed[2], and one of the mostly used is [6]

$$f(x) = 1 - (2x-1)^{2p}, \tag{3}$$

[1]Nowadays, there are several techniques to realize memristors by using different materials (see e.g. [18]).
[2]A linear approximation is presented in [20], with a nonlinear form in [21] (see also [22, 15]).

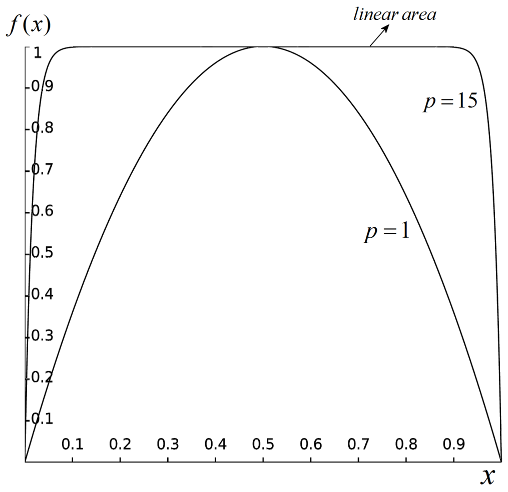

Figure 3: Graphs of window function $f(x) = 1 - (2x - 1)^{2p}$ for $p = 1$ and $p = 15$.

with p being a positive integer. The behavior of this function on some subintervals can be linear or nonlinear, depending on p (Fig. 3), an important parameter for calculating the fractional resistance of the ideal memristor.

In order to build the SCC, Muthuswamy and Chua [23] used a more general vector window function (1b), $f(x, i_M) = i_M - \alpha x - i_M x$, and a nonlinear memristance (1a), $R(x) = \beta(x^2 - 1)$, with α and β being real parameters. This kind of generalization of the ideal memristor (1a)-(1b) is called a *memristive system*[3]:

$$M : \begin{cases} V_M = R(x) i_M = \beta(x^2 - 1) i_M, & \text{(4a)} \\ \dot{x} = f(x, i_M) = i_M - \alpha x - i_M x. & \text{(4b)} \end{cases}$$

Remark 1. *Compared to other memristor-based chaotic circuits, the autonomous SCC with $R(x)$ given by* (4a)-(4b) *is bounded-input bounded-output* [1]. *Also, the memristive system* (4a)-(4b) *makes possible the existence of a chaotic single-loop circuit with three independent state variables.*

Sometimes, physical phenomena are modeled more accurately by differential equations of fractional order than by integer-order equations [24]. Therefore, it is not at all surprising that the combined use of fractional calculus and impulsive systems was implemented in circuit experiments (see e.g. [19, 25]).

If derivatives of the Caputo type are used to model these dynamical systems, the initial conditions can be formulated just as for classical ordinary differential equations, $x(0) = x_0$ [26]. Given a function $f : \mathbb{R}^n \to \mathbb{R}$, $n \geq 1$, Caputo's differential operator of order $0 < q \leq 1$ with respect to the starting point 0, applied to f, is defined as (see e.g. [27])

$$D_*^q f(t) = \frac{1}{\Gamma(1-q)} \int_0^t (t-s)^{-q} f'(s)\, ds,$$

[3] In [1], it is mentioned that other forms for R have already been or could be chosen.

where Γ is Euler's Gamma function.

On the other hand, impulsive fractional differential equations represent a framework for mathematical modeling of real-world problems. Significant progress has been made in the theory of impulsive fractional differential equations [28].

In this paper the following impulsive Initial Value Problem (IVP) of fractional order is considered:

$$\begin{aligned} &D_*^q x(t) = f(x), \quad \text{for } t \in I = [0,T],\ t \neq t_k,\ k = 1,2,...,\ 0 < q \leq 1, \\ &\Delta x|_{t=t_k} = I_k(x(t_k^-)),\ k = 0,1,2,... \\ &x(0) = x_0, \end{aligned} \tag{5}$$

where $I_k : \mathbb{R} \to \mathbb{R}$, $x_0 \in \mathbb{R}$, $0 = t_0 < t_1 < ...$, $\Delta x|_{t=t_k} = x(t_k^+) - x(t_k^-)$, $x(t_k^+) = \lim_{h \downarrow 0} x(t_k + h)$ and $x(t_k^-) = \lim_{h \uparrow 0} x(t_k - h)$ represent the right and left limits of $x(t)$ at $t = t_k$, with a generally nonlinear continuous function $f : \mathbb{R}^n \to \mathbb{R}^n$.

In other words, the IVP is subject to some impulsive effects at fixed time instants (points of jump). The IVP (5) should be read as follows:

- For $t \neq t_k$, $k = 0,1,...$, the solution is given by the equation $D_*^q x(t) = f(x)$;
- For $t = t_k$, the solution $x(t)$ jumps so that $x(t_k^-) = x(t)$ and $x(t_k^+) = x(t) + \Delta x(t_k)$;
- After a jump instant, t_k, the solution is given by the following IVP: $D_*^q x(t) = f(x)$, for $t_k < t < t_{k+1}$.

Due to the nonlinearity of f, the underlying system modeled by (5) may behave chaotically. However, by choosing an adequate time partition $t_1, t_2, ...$, and impulses $\Delta x(t_k)$, the chaotic behavior can be controlled. While chaos control is matured for integer-order impulsive systems today [29], it is still relatively new in the fractional order settings (see e.g. [30]).

This kind of algorithm is useful in certain chemical and biological systems, electrical circuits, particularly when system parameters are unaccessible, leading to the failure of the OGY method [31] and other similar control strategies.

In this paper, aided by computer simulations, we show that there are more general impulsive-like methods to suppress chaotic behaviors. Consequently, we show that chaos suppression can be achieved with constant but different impulses applied to one or several system state variables. For this purpose, by drawing a bifurcation diagram with impulses considered as bifurcation parameters, we found relatively large connected subintervals of impulsive controls, where the suppression of chaos can be realized.

The rest of the paper is structured as follows. In Section 2, a fractional-order variant of the autonomous SCC is derived and a general impulsive algorithm to suppress the chaotic behavior is described. Numerical results are presented in Section 3 and, finally, conclusions are drawn in the last section.

2. Autonomous SCC model of fractional order and chaos suppression

For a fractional-order ($0 < q \leq 1$) capacitor and inductor, the $i-v$ relations, necessary for deriving the mathematical model of the current-controlled SCC of fractional order, are given respectively as follows (see e.g. [32]):

$$\begin{aligned} i_C(t) =& C\, D_*^q v_C(t), \\ v_L(t) =& L\, D_*^q i_L(t). \end{aligned}$$

Then, referring to the circuit presented in Fig. 1, based on a capacitor, an inductor and a memristor system of fractional order q_1, q_2 and q_3, respectively, Kirchhoff's voltage law on the loop gives

$$v_C + L\, D_*^{q_2} i_L - R\, i_M = 0.$$

If one considers Kirchhoff's current law $i_M = -i_L$, and the equations of the memristive system (4a)-(4b), then the mathematical model of the autonomous SCC of incommensurate fractional order, $(q_1, q_2, q_3)^T$, as a counterpart of the integer-order circuit presented in [1], can be derived as[4]

$$\begin{aligned} D_*^{q_1} v_C &= \frac{i_L}{C}, \\ D_*^{q_2} i_L &= -\frac{1}{L}(v_C + \beta\, i_L - \beta\, x^2 i_L), \\ D_*^{q_3} x &= -i_L - \alpha x + i_L\, x. \end{aligned} \tag{6}$$

Using a dimensionless variables substitution: $x_1 := v_C$, $x_2 := i_L$ and $x_3 := x$, and letting $C = 1$, $L = 3$, $\alpha = 0.6$, as given in [1], system (6) can be transformed into the following dimensionless form:

$$\begin{aligned} D_*^{q_1} x_1 &= x_2, \\ D_*^{q_2} x_2 &= -\frac{1}{3}(x_1 + \beta x_2 - \beta x_3^2 x_2), \\ D_*^{q_3} x_3 &= -x_2 - 0.6 x_3 + x_2 x_3. \end{aligned} \tag{7}$$

Remark 2. *System* (7) *has the same form as its integer-order counterpart presented in* [1]*, with the only difference being Caputo's fractional derivative. However, equations* (4a)-(4b) *of the memristive system are adopted as defined for the integer-order system. Therefore, a more realistic approach for fractional-order systems could be considered.*

Now, consider the ideal memristor equations (1a)-(1b), (2), (3)*, and the window function f in its linear window (where $f(x) = 1$, see Fig. 3). The following expression for memristor resistance R, depending on the input voltage and time, can be deduced* [25]*:*

$$R(t) = \left(R_{in}^{q+1} \mp q(q+1)kR_\Delta \int_0^t (t-\tau)^{q-1} v(\tau)\, d\tau \right)^{\frac{1}{q+1}},$$

where $R_\Delta = R_{off} - R_{on}$ and R_{in} are some initial values.

Obviously, with this form of R, the fractional-order equations (7) *become more complicated. Therefore, due to the simplicity of the canonical form* (7)*, only a simplified model is studied here.*

Consider next the impulsive system (5) for the case of a chaotic system (7). The existence of solutions (piecewise continuous functions satisfying (5)), was proved in e.g. [28, 34].

Generally, in stabilizing chaotic systems of integer or fractional order, it is based on adaptive or feedback controls, justified by the Lyapunov stability. The designed impulses are variables depending on the system dynamics at every time instant t_k, and are applied at the same time instants.

In this paper, we consider the case of impulses, denoted by Δx_i, applied periodically, but at same or different time moments, under the following assumptions:

[4] In [33], the stability and dynamic behavior of the autonomous SCC are studied for the commensurate case.

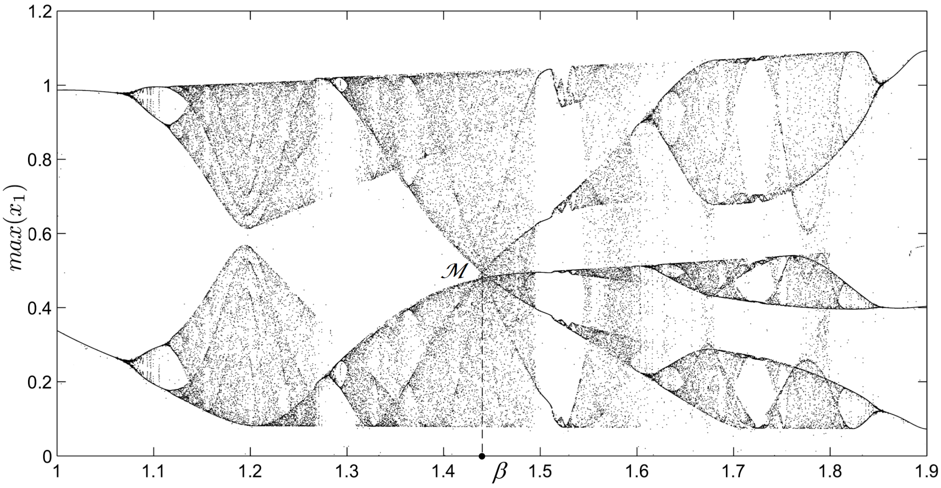

Figure 4: Bifurcation diagram of the autonomous SCC of fractional order (7).

- Impulses are applied to $1 \leq N \leq n$ variables x_i, at time instants t_k^i, $i \in \{1, 2, ..., N\}$, $k = 0, 1, ...$;
- The variable x_i receives impulses Δx_i at the instants t_k^i, where $i \in 1, 2, \cdots, N, k = 0, 1, \cdots$. The impulses can be applied either simultaneously (i.e. t_k^i is the same for all considered N variable) or at different time instants (i.e. $t_k^i \neq t_k^j$ if $i \neq j$);
- Time interval I is equidistantly partitioned, but possibly differently, for each considered variable x_i, $i \in \{1, 2, ..., N\}$, so that $t_{k+1}^i - t_k^i = \delta x_i$ for all k.

To the best of our knowledge, there are no studies to determine the required parameters for this kind of impulsive problems of fractional order. Due to the commonly-known impossibility of analytical derivations, Δx_i and δx_i are determined numerically aided by computer simulations.

Conceptually, the impulsive problem (5) can be written as follows:

$$x_i(t_k^{i+}) = x_i(t_k^{i-}) + \Delta x_i \text{ after every } \ \delta x_i \text{ and all } k, \quad i \in \{1, 2, ..., N\}, \quad N \leq n, \tag{8}$$

which means that after every δx_i time interval, the variable x_i, $i \in \{1, 2, ..., N\}$, is subject to an impulsive change of Δx_i.

3. Numerical results

As numerical examples, consider system (7) for the non-commensurate case with $q = (0.98, 0.99, 0.995)^T$ and β chosen nearby the coordinate of the point $\mathcal{M}$, i.e. 1.43 (a Misiurewicz-like point), which yields

$$\begin{aligned} D_*^{0.98} x_1 &= x_2, \\ D_*^{0.99} x_2 &= -\frac{1}{3}(x_1 + \beta x_2 - \beta x_3^2 x_2), \\ D_*^{0.995} x_3 &= -x_2 - 0.6 x_3 + x_2 x_3. \end{aligned} \tag{9}$$

Its complex behavior can be seen from the bifurcation diagram in Fig. 4. With $\beta = 1.43$, the system provides most complex chaotic dynamics. For this choice of β, the chaotic attractor fills densely a subspace of the phase space (Fig. 5). In contrast, for the attractors corresponding to different β values, there are some regions in the phase space which are never visited by the underlying attractor. Therefore, chaotic attractors are "less" chaotic for $\beta \neq 1.43$ (as is considered in [1], for example).

The values of q_1, q_2, q_3 have been chosen close to one, in order to retain as much as possible the chaotic feature of its integer-order counterpart (as is well known, chaos tends to vanish once the system order diminishes).

In order to verify the obtained results, phase plots and histograms (for the first state variable x_1) are shown, where transients have been neglected in phase plots. Impulse values are obtained from the bifurcation diagram with impulses considered as bifurcation parameters and with a fixed δx_1. From this diagram, one can deduce the values of Δx_1 for which the system evolves along a stable cycle.

The numerical integration of (7) was realized with the Adams-Bashforth-Moulton method for fractional-order equations [35], with the step size $h = 0.002$, while the integration interval was set as $I = [0, 300]$, except for the case of $\delta = -0.00062$ when a longer period of time is necessary to eliminate transients.

For each variable x_i, the time interval δx_i is set as multiple of h, so that in the underlying time partition $t_0^i, t_1^i, ...$, the distance between consecutive points t_k^i and t_{k+1}^i, $k = 0, 1, ...$, is $\delta x_i = |t_{k+1}^i - t_k^i| = m\,h$, where m is a positive integer.

Remark 3. *It should be mentioned that the obtained results here depend on the characteristics of the numerical methods used to solve the underlying impulsive IVP of fractional order, and the step size h. Based on extensive numerical simulations, it is realized that by the use of Adams-Bashforth-Moulton's method within the usual range of size h, for example* $(0.001, 0.004)$*, the results remain*

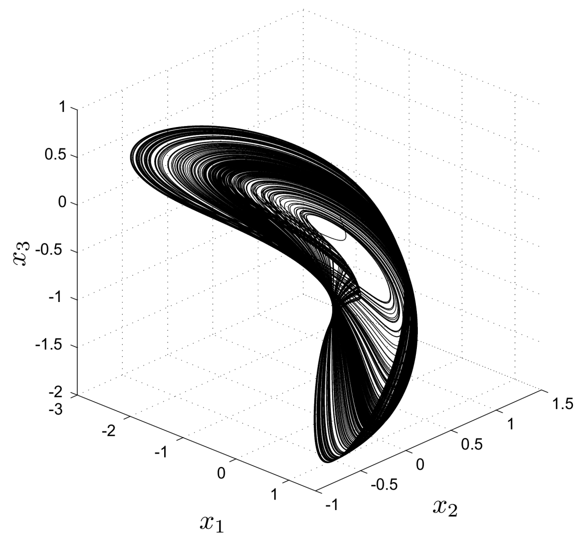

Figure 5: Chaotic attractor of the autonomous SCC (7) for $\beta = 1.43$.

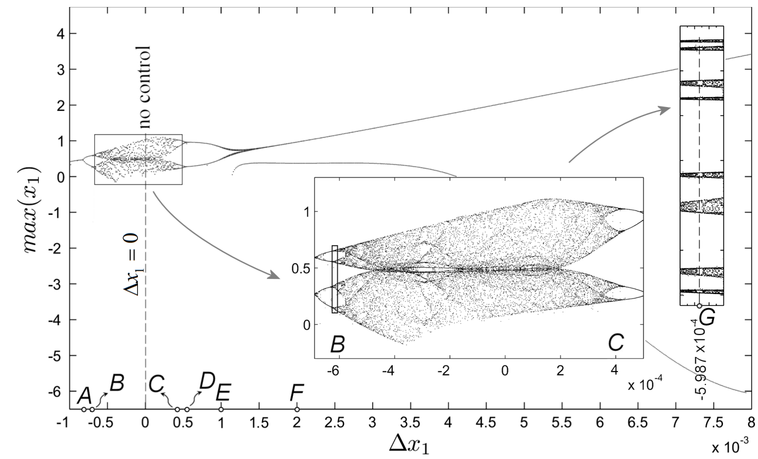

Figure 6: Bifurcation diagram of x_1 for the autonomous SCC of fractional-order (7) using Δx_1 as bifurcation parameter, and some zoomed regions.

essentially unchanged. Another potential issue is the rounding errors, e.g. from the repeating (recurring) decimals in (7), $1/3 = 0.33...$ *(as deduced in* [1]*).*

Next, the most significative results are presented for applying (negative and positive) impulses to one, two and all variables of the system under control.

- First, consider the case of a single variable x_1 ($N = 1$), in which the impulse Δx_1 is applied at every $\delta x_1 = h$, i.e. x_1 is modified with Δx_1 in every integration step h. The bifurcation diagram, which plots the relative maxima of x_1 versus Δx_1, for $\Delta x_1 \in \Delta = (-0.001, 0.008)$ (Fig. 6)[5], indicates the intervals where every applied value Δx_1 ensures chaos suppression. As can be seen, there exists an interval BC, with $B \approx -6 \times 10^{-4}$ and $C \approx 4 \times 10^{-4}$, within which there are some chaos suppression intervals (intervals for which Δx_1 ensures chaos suppression), merging with chaotic intervals (where chaos is not suppressed). It resembles a period-doubling bifurcations connected with a reverse bifurcation cascade of the logistic map. For every Δx_1 outside the BC value interval, chaos can be suppressed. As expected, at $\Delta x_1 = 0$ (no impulses), the system evolves chaotically. The probability to find impulses Δx_1 in Δ such that the system behaves regularly, is more than 90% which is pretty large.
  - With $\Delta x_1 = -0.00062$ (point A in the bifurcation diagram in Fig. 6), the chaotic behavior is suppressed and the system evolves along a complicated higher-periodic stable cycle, as shown in Fig. 7. Histogram highlights the fact that Δx_1 is chosen on the right to a period-doubling bifurcation point.
  - With $\Delta x_1 = 0.0005$ (point D in the bifurcation diagram in Fig. 6), the chaotic behavior disappears and a stable cycle appears (Fig. 8). As for $\Delta x_1 = -0.00062$, the value $\Delta = 0.0005$ is chosen near a bifurcation point, as underlined by histogram's peaks.

[5]Values outside this range for Δx_1 present no interest from the physical point of view. Also, values smaller than -1×10^{-3} determine system instability.

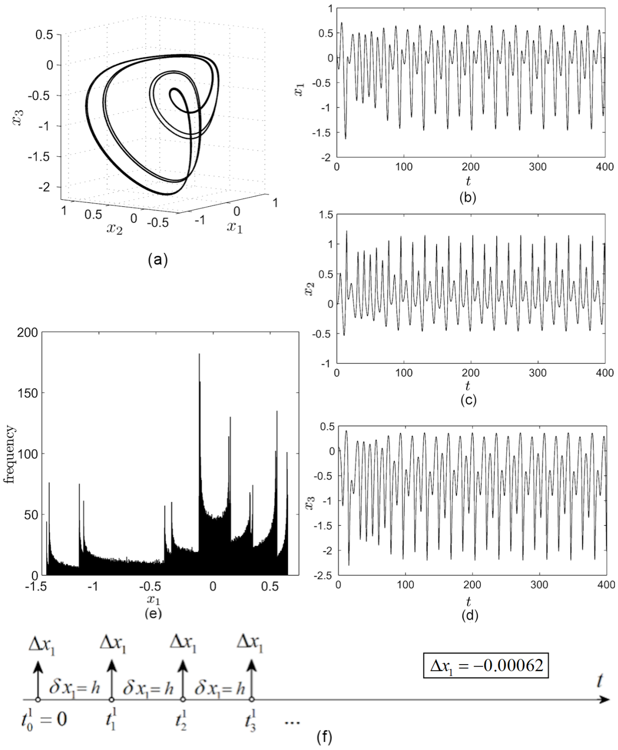

Figure 7: Chaos suppression with impulses applied to a single variable x_1, where $\delta x_1 = h$ and $\Delta x_1 = -0.00062$ (point A in the bifurcation diagram in Fig. 6); a) Phase plot; b-d) Time series; e) Histogram of x_1 component; f) Impulse time instants for x_1 (sketch).

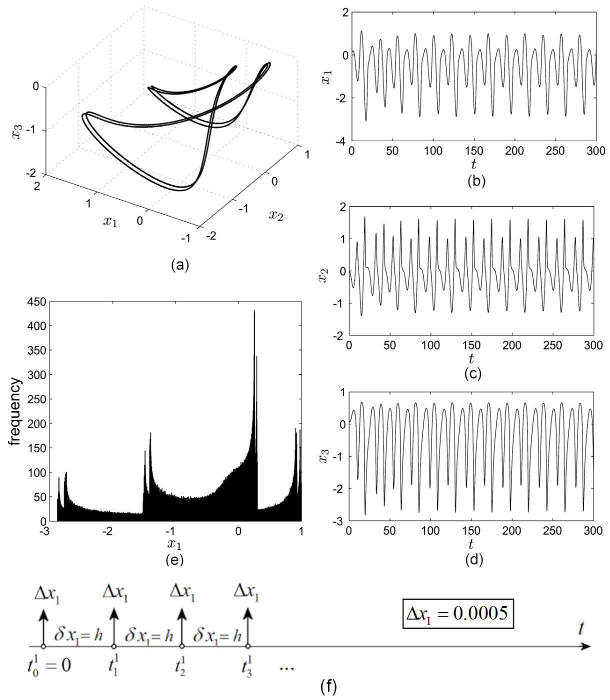

Figure 8: Chaos suppression with impulses applied to a single variable x_1, where $\delta x_1 = h$ and $\Delta x_1 = 0.0005$ (point D in the bifurcation diagram in Fig. 6); a) Phase plot; b-d) Time series; e) Histogram of x_1 component; f) Impulse time instants for x_1 (sketch).

  - With $\Delta x_1 = 0.001$ (point E in the bifurcation diagram in Fig. 6), the chaotic behavior is regularized, as shown in Fig. 9. The period of the stable cycle reduces.
  - With $\Delta x_1 = 0.002$ (point F in the bifurcation diagram in Fig. 6), the chaotic behavior is stabilized, as shown in Fig. 10. Similarly, the period of the stable cycle reduces.

- If one considers $N = 2$ variables, e.g. x_1 and x_3, with the corresponding impulses $\Delta x_1 = 0.001$ and $\Delta x_3 = -0.002$, applied every $\delta x_1 = 2\,h$ and $\delta x_3 = 5\,h$ moments respectively, one obtains the stable cycle in Fig. 11.

- If one applies impulses $\Delta x_1 = 0.004$, $\Delta x_2 = -0.001$ and $\Delta x_3 = -0.002$ to all variables, every $\delta x_1 = 8\,h$, $\delta x_2 = 5\,h$ and $\delta x_3 = -0.002$ moments respectively, one obtains the stable cycle shown in Fig. 12, which resembles the cycle obtained in the above case, with $N = 2$ variables.

As can be seen from the presented results, either positive or negative impulses can be applied to suppress the chaotic behavior.

Remark 4. *In* [36]*, the stable regions controlling chaos in Chua's oscillator using impulsive control are connected. In the present case here, there are stable subintervals for* Δx_1*, where chaos suppression can be realized, interweaving with unstable subintervals, where chaos cannot be suppressed (see*

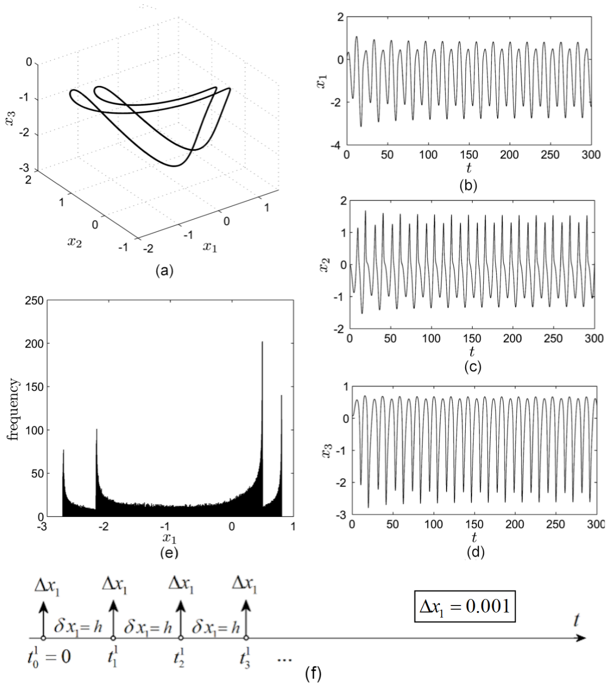

Figure 9: Chaos suppression with impulses applied to a single variable x_1, where $\delta x_1 = h$ and $\Delta x_1 = 0.001$ (point E in the bifurcation diagram in Fig. 6); a) Phase plot; b-d) Time series; e) Histogram of x_1 component; f) Impulse time instants for x_1 (sketch).

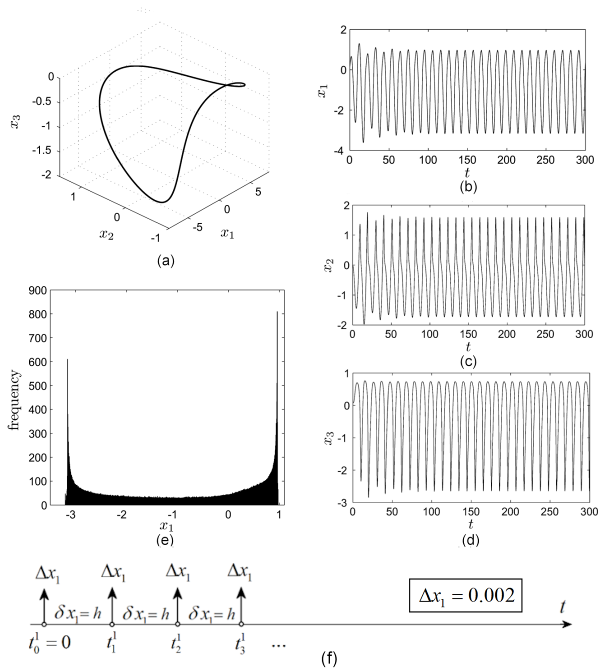

Figure 10: Chaos suppression with impulses applied to a single variable x_1, with $\delta x_1 = h$ and $\Delta x_1 = 0.002$ (point F in the bifurcation diagram in Fig. 6); a) Phase plot; b-d) Time series; e) Histogram of x_1 component f) Impulses time instants for x_1 (sketch).

for example, based on the point G in Fig. 6 *where* $\Delta_1 = 5.987 \times 10^{-4}$*, a stable cycle with a higher period is obtained as shown in* Fig. 13*).*

4. Conclusion and discussion

We have shown that the chaotic behavior of a simplest autonomous SCC of non-commensurate fractional order can be suppressed by applying periodic impulses. The impulse values can be different and can be applied to one or several state variables.

To determine the impulses, bifurcation diagrams can be utilized, with impulses considered as bifurcation parameters.

The difficulty to realize the impulsive control (5) in electronic circuit lies in the fact that a direct and impulsive change of the state variables is required. Unlike other state feedback control, the control signal does not act onto the system equation, namely the circuit in concern. Taking a capacitor in a circuit as example, to change its voltage as specified by (5), it requires an injection of electrons leading to a sudden change of the voltage, without going through the circuit. This is not generally on-shelf available, but some models of impulsive electronic devices have been suggested [37] and it is technically possible in the light of physics. For example, a single electron tunneling junction can work as a capacitor, and based on the Coulomb blockade, a single electron tunneling through the barrier can cause a sudden voltage jump at the junction capacitor. In contrast, for

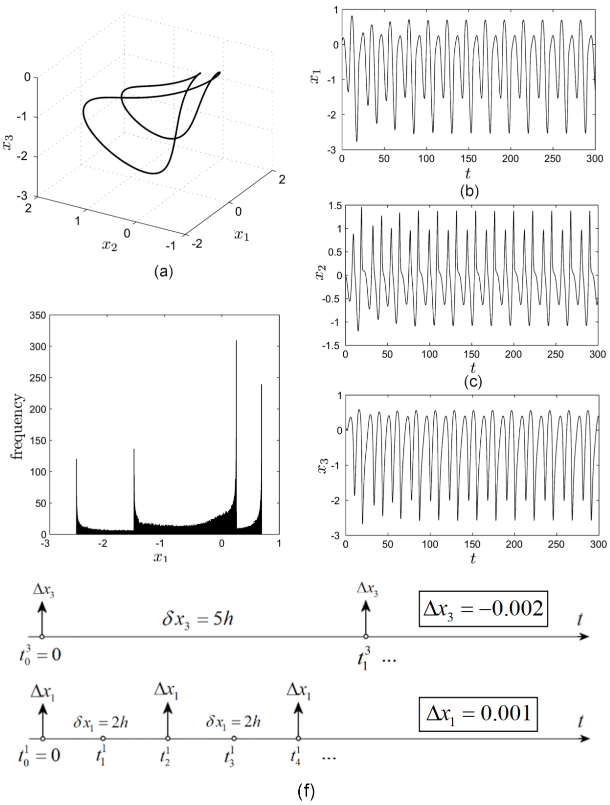

Figure 11: Chaos suppression with impulses applied to two variables, x_1 and x_3, with $\delta x_1 = 2\,h$, $\delta x_3 = 5\,h$, $\Delta x_1 = 0.001$, $\Delta x_3 = -0.002$; a) Phase plot; b-d) Time series; e) Histogram of the x_1 component f) Impulse time moments for x_1 and x_3 (sketch).

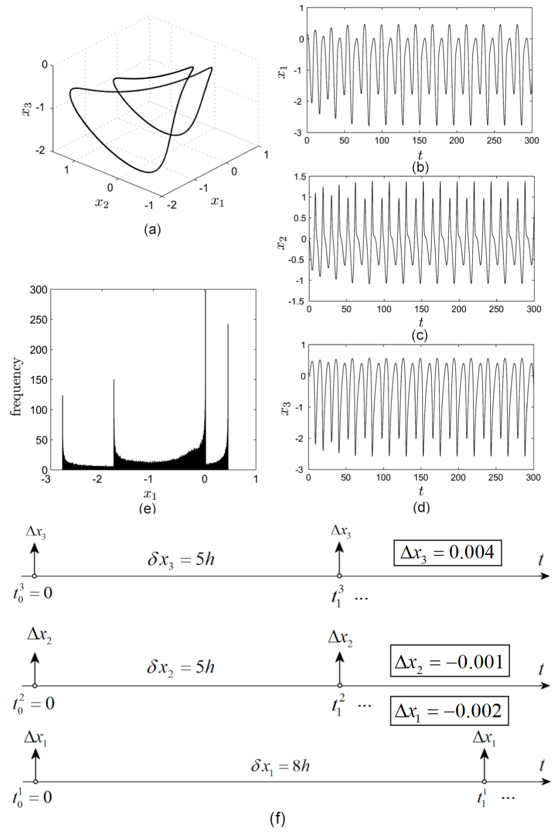

Figure 12: Chaos suppression with impulses applied to all variables, x_1, x_2 and x_3, with $\delta x_1 = 8\,h$, $\delta x_2 = 5\,h$, $\delta x_3 = 5\,h$, $\Delta x_1 = 0.004$, $\Delta x_3 = -0.001$, $\Delta x_3 = -0.002$; a) Phase plot; b-d) Time series; e) Histogram of the x_1 component f) Impulse time moments for x_1, x_2 and x_3 (sketch).

biological systems, which have also been frequently modeled by fractional differential equations [38, 39], it is relatively easier to realize the impulsive control (5) by external injection and operation without affecting other states. This line of thinking will be further investigated in the future.

Acknowledgement This project was supported by the Hong Kong Research Grants Council under the GRF Grant CityU11201414.

References

[1] B. Muthuswamy, L.O. Chua, Int. J. Bifurcat. Chaos 20(5) (2010) 1567 DOI:10.1142/S0218127410027076.
[2] L.O. Chua, Int. J. Bifurcat. Chaos (2005) 3435 DOI:10.1142/S0218127405014337
[3] L.O. Chua, IEEE Trans. Circuit Th. CT 18 (1971) 507 DOI:10.1109/TCT.1971.1083337.
[4] A. Thomas, J. Phys. D: Appl. Phys. 46 (2013) 093001 DOI:10.1088/0022-3727/46/9/093001.
[5] D.B. Strukov, G.S. Snider, G.R. Stewart, R.S. Williams, Nature 453 (2008) 80 DOI:10.1038/nature06932.

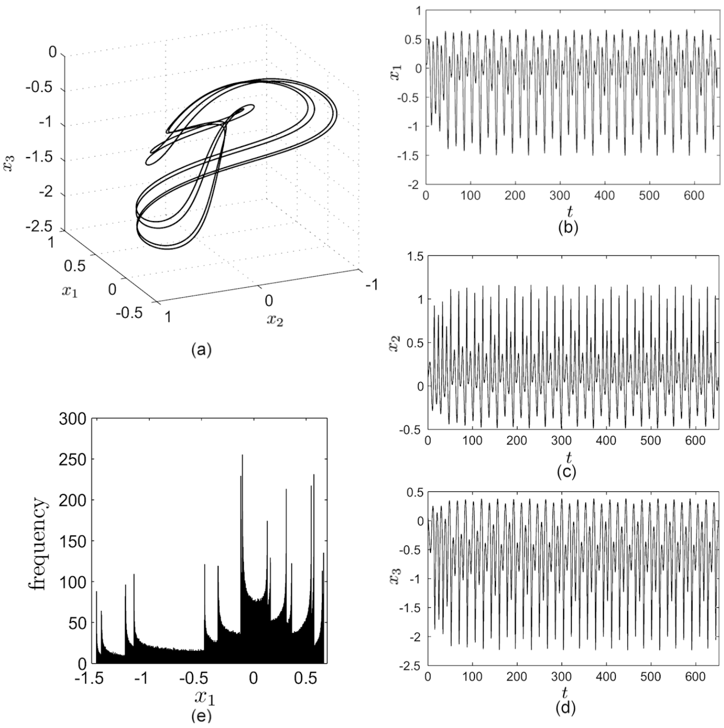

Figure 13: Chaos suppression with impulses applied to a single variable x_1, $\delta x_1 = h$ and $\Delta x_1 = -5.987 \times 10^{-4}$ (point G in the bifurcation diagram in Fig. 6); a) Phase plot; b-d) Time series; e) Histogram of the x_1 component.

[6] Z. Biolek, D. Biolek, V. Biolkova, Radioengineering 18 (2009) 210.

[7] Q. Xia, W. Robinett, M.W. Cumbie, N. Banerjee, T.J. Cardinali, J.J. Yang, W. Wu, X. Li, W.M. Tong, D.B. Strukov, G.S. Snider, G. Medeiros-Ribeiro, R.S. William, Nano Lett. 9 (2009) 3640 DOI:10.1021/nl901874j.

[8] E. Linn, R. Rosezin, C. Kuegeler, R. Waser, Nature Mater. 9 (2010) 403 DOI:10.1038/nmat2748.

[9] J.J. Yang, D.B. Strukov D.R. Stewart, Nat. Nanotechnol. 8 (2013) 13, DOI:10.1038/nnano.2012.240.

[10] J.J Yang, M.X Zhang, J.P Strachan, F. Miao , M.D. Pickett, R.D. Kelley, G. Medeiros-Ribeiro, R.S. Williams, Appl. Phys. Lett. 97 (2010) 232102, DOI: 10.1063/1.3524521

[11] A. Adamatzky, L.O. Chua, Memristor Networks, Springer, 2014.

[12] G.K. Johnsen, J. Electr. Bioimped. 3 (2012) 20 DOI: 10.5617/jeb.305.

[13] J.M. Tour, T. He, Nature 453 (2008) 42 DOI:10.1038/453042a.

[14] D. Wang, Z. Hu, X. Yu, J. Yu, ?A PWL model of memristor and its application example,? International Conference on Communications, Circuits and Systems, 2009. ICCCAS 2009, pp. 932–934, July 2009.

[15] O. Kavehei, A. Iqbal, Y.S. Kim, K. Eshraghian, S.F. Al-Sarawi, D. Abbot, Proc. R. Soc. A 466 (2010) 2175 DOI:10.1098/rspa.2009.0553.

[16] Z. Yin, H. Tian, G. Chen, L.O. Chua, What are Memristor, Memcapacitor, and Meminductor?, IEEE T. Circuits-II 62 (2015) 402 DOI:10.1109/TCSII.2014.2387653.

[17] L.O. Chua, S.M. Kang, Memristive Devices and Systems. Proceedings of the IEEE 64, 209?223 (1976).
[18] Z.J. Chew, L. Li, Mater. Lett. 91 (2013) 298 DOI:10.1016/j.matlet.2012.10.011.
[19] A.G. Radwan, M.A. Zidan, K.N. Salama, On the Mathematical Modeling of Memristors, Microelectronics (ICM), 2010 International Conference on , 19-22 Dec. 2010 284 - 287 DOI:10.1109/ICM.2010.5696139.
[20] S. Benderli, T. A. Wey, Electron. Lett. 45 (2009), 377.
[21] Y.N Joglekar, S.J. Wolf, Eur. J. Phys. 30 (200) 661 DOI:10.1088/0143-0807/30/4/001.
[22] X. Mu, J. Yu, S. Wang, Int. J. Numer. Model. 28 (2015) 96 DOI: 10.1002/jnm.1987.
[23] L.O. Chua, S. M. Kang, Proc. IEEE 64, (1976) 209 DOI:10.1109/PROC.1976.10092.
[24] R. Hilfer, (ed.): Applications of Fractional Calculus in Physics. World Scientific, Singapore (2000).
[25] M.E. Fouda, A.G. Radwan, Journal of Fractional Calculus and Applications, 4 (2013) 1.
[26] N. Heymans, I. Podlubny, Rheologica Acta, 45 (2006) 765 DOI:10.1007/s00397-005-0043-5.
[27] K. Diethelm, The Analysis of Fractional Differential Equations, An Application-Oriented Exposition Using Differential Operators of Caputo Type, Springer-Verlag, Berlin Heidelberg, 2010.
[28] M. Benchohra, J. Henderson, S. K. Ntonyas, Impulsive Diffrential Equations and Inclusions, vol. 2, Hindawi Publishing Corporation, New York, NY, USA, 2006.
[29] M.A. Matias, J Güémez, Phys. Rev. Lett. 72 (1994) 1455 DOI:http://dx.doi.org/10.1103/PhysRevLett.72.1455.
[30] Q.-S. Zhong, J.-F. BAO, Y.-B. Yu, X.-F. Liao, Chin. Phys. Lett. 25 (2008) 2812 DOI:10.1088/0256-307X/25/8/022.
[31] Ott, E., Grebogi, C., J. Yorke, Phys. Rev. Lett., 64 (1990), 1196 DOI http://dx.doi.org/10.1103/PhysRevLett.64.1196.
[32] I. Petráš, Y. Chen, C. Coopmans, Fractional-order Memristive Systems, Conference on Emerging Technologies and Factory Automation, ETFA 2009, September 22-25, 2008, Palma de Mallorca, Spain.
[33] D. Cafagna G. Grassi, Nonlinear Dyn. 70 (2012) 1185 DOI:10.1007/s11071-012-0522-z.
[34] L. Mahto, S. Abbas, A. Favini, International Journal of Differential Equations 2013 (2013) 704547 DOI:10.1155/2013/704547.
[35] K. Diethelm, N.J. Ford, A.D. Freed, Nonlinear Dynam. 29 (2002) 3 DOI:10.1023/A:1016592219341.
[36] T. Yang, L.O. Chua, IEEE T. Circuits-I 44 (1997) 976 DOI:10.1109/81.633887.
[37] T. Yang, ?Applications to nanoelectronics,? Chap 11 in Impulsive Control Theory, Springer, 2001.
[38] F.A. Rihan, Abstr. Appl. Anal. (2013), article 816803 DOI: http://dx.doi.org/10.1155/2013/816803
[39] V.-D.-L. Cruz, Commun. Nonlinear Sci. 24 (2015), 75 DOI:10.1016/j.cnsns.2014.12.013.